the Anti–Lung Cancer Association (ALCA), a for-profit organization for lung cancer screening.[20,21] Each screening consisted of a low-dose helical CT examination, chest radiography, and cytologic sputum studies. During this period, a total of 15,938 low-dose helical CT examinations were performed in 2052 ALCA members. Among the low-dose helical CT examinations, a total of 1566 CT examinations were judged as having abnormal findings requiring further examination. Sixty-seven cases of lung cancer (peripheral-type lung cancer, 61; hilar-type lung cancer, 6) were detected during the ALCA lung cancer screening project. Out of these 67 cases, 51 cases (76%) were pathologic stage IA. The treatments used in the 67 cases were as follows: surgery (n = 55), radiotherapy (n = 5), radiotherapy and chemotherapy (n = 2), chemotherapy (n = 4), and photodynamic therapy (n = 1). Among the patients with peripheral nodules detected by the low-dose helical CT examinations performed every 6 months, the patients with histologically diagnosed nodules exhibiting pGGO larger than 5 mm in diameter at the time of the first thin-section CT and followed-up by thin-section CT for more than 6 months were enrolled in the current study.

CT Scanning Conditions

A TCT900S Superhelix CT scanner (Toshiba Medical Inc., Tokyo, Japan) was used for all of the examinations. Low-dose helical CT screening was performed under the following conditions: 120 kV, 50 mA, beam width of 10 mm, 1 rotation of the x-ray tube per second, and a table speed of 20 mm per second (pitch 2:1). Reconstruction was performed at intervals of 10 mm. The CT images were displayed on a monitor with a window width of 2000 HU and a window level of −700 HU. If newly developed nodules were identified, thin-section CT examinations were performed under the following conditions: 120 kV, 250 mA, beam width of 2 mm, 1 rotation of the x-ray tube per second, and a table speed of 2 mm per second (pitch 1:1). Reconstruction was performed at intervals of 2 mm using a thin-section CT algorithm.

Evaluation of pGGO Progression Patterns

The progression patterns were classified based on changes in the size and density of the pGGOs on the thin-section CT images. The study period was divided into 2 phases: the unidentified phase (ie, the period prior to the first thin-section CT scan) and the follow-up phase (ie, the period after the first thin-section CT scan). CT images of the pGGOs in the unidentified phase were reviewed independently by 4 physicians (R.K., M.K., H.O., K.E.), who are diagnostic experts in chest radiology, and by 1 radiologist (M.K.). CT findings were adopted as positive findings if 3 of more of the doctors agreed. After the independent reviews, we decided by consensus as to how many pGGOs were newly developed or had arisen from inconspicuous nodules during the helical CT screening period. In the follow-up phase, the size of the pGGOs was measured with a pair of calipers on the thin-section CT images obtained during the initial scan and the final scan by consensus of 2 diagnostic experts (R.K., M.K.) to assess doubling time. The size of the lesion was evaluated using measurements that passed through the center of the lesion. Size was defined as the average of the length and width of the lesion. Doubling times were calculated using the Schwartz equation.[22] The density of faint opacities was evaluated visually on the thin-section CT images obtained during the follow-up phase. pGGO was defined as a homogeneous GGO, and mixed GGO was defined as a GGO with a solid component.

Pathologic Classification of Adenocarcinomas

The histologic findings of the adenocarcinomas were classified according to the criteria of the World Health Organization (WHO)[23] and the criteria of Noguchi et al.[24] The classification system for replacement growth patterns developed by Noguchi et al is as follows: type A (localized bronchioloalveolar carcinoma; LBAC), type B (LBAC with foci of collapsed alveolar structure), and type C (LBAC with foci of active fibroblastic proliferation).

RESULTS

Patient Characteristics

Eight patients with pGGOs (6 men and 2 women) were enrolled in the current study (Table 1). The patients ranged in age from 49 to 69 years (mean, 64 years). With regard to smoking history, 3 patients were nonsmokers, 4 were ex-smokers, and 1 was a current smoker. Four of these 8 pGGO patients were not apparent during the initial screening and became apparent during the screening period, and 3 of the other 4 pGGO patients with inconspicuous opacities visible in retrospect during the initial screening became apparent later. In 1 other case, a conspicuous opacity and multiple old tuberculosis lesions were observed during the initial CT screening. The locations of the pGGOs were as follows: right upper lobe (n = 4), right lower lobe (n = 1), left upper lobe (n = 1), and left lower lobe (n = 2).

Clinical Course

The period between the first visible nodule of a pGGO on a thin-section CT image and the first visible opacity on a helical CT screening image when viewed retrospectively ranged from 13 to 46 months (mean, 22 months) (Table 1). The period between the first thin-section CT examination and the surgery ranged from 7 to 39 months (mean, 19 months). The interval between the last thin-section CT examination and surgery ranged from 1 to 98 days (mean, 32 days).

Histology of GGOs

Seven patients had bronchioloalveolar carcinoma (BAC), defined as noninvasive by the WHO classification in 1999, and 1 had an adenocarcinoma with mixed subtypes (Table 1). Based on Noguchi's classification for small adeno-

© 2004 Lippincott Williams & Wilkins

TABLE 1. Clinical Characteristics and Histology of Ground-Glass Opacities

Case No.	Sex	Age at Detection (Years)	Smoking Index	Development	Lobe	Period Between: First Visible and the First TS-CT (Months)*	Period Between: The First TS-CT and Surgery (Months)*	Period Between: The Last TS-CT and Surgery (Days)	Histology: WHO Classification	Histology: Noguchi Type
1	M	69	1300	New	RU	41	13	1	Ad	C
2	M	69	800 (ex)	New	RU	13	39	36	BAC	B
3	F	66	Non	New	LL	13	14	33	BAC	A
4	M	66	450 (ex)	New	LU	18	26	98	BAC	A
5	F	65	Non	ic	LL	46	28	13	BAC	B
6	M	69	800 (ex)	ic	RU	21	12	13	BAC	A
7	M	49	515 (ex)	ic	RU	14	10	6	BAC	A
8	M	63	Non	c	RL	13	7	57	BAC	B

Non, nonsmoker; ex, ex-smoker; ic, inconspicuous; c, conspicuous; RU, right upper lobe; LU, left upper lobe; LL, left lower-lobe; TS-CT, thin-section CT; BAC, bronchioloalveolar carcinoma; Ad, adenocarcinoma.
*Number of months was rounded.

carcinomas, the pGGOs consisted of 4 cases of type A and 2 cases of type B while the mixed GGOs consisted of 1 case of type B and 1 case of type C (Tables 1, 2). All the lung cancers were diagnosed at pathologic stage IA.

Progression of pGGOs

The period between the first thin-section CT and the final thin-section CT examinations ranged from 6 to 37 months (mean, 17 months) (Table 3). The opacities ranged in size from 6.5 mm to 17 mm (mean, 10 mm) at the time of the first thin-section CT examination and from 7 mm to 16.5 mm (mean, 10.5 mm) at the time of the final thin-section CT examination. The progressions of 8 opacities in the follow-up phase were classified into 3 types: increasing in size (Increasing type, n = 5), decreasing in size and the appearance of a solid component (decreasing type, n = 2), and stable in size and increasing in density (density type, n = 1). In addition, the decreasing type was classified into 2 subtypes: a rapid-decreasing type (case 1, Fig. 1; decrease in size at the time of the 6-month follow-up) and a slow-decreasing type (case 2, Fig. 2; decrease after follow-up for more than 1 year). All but 1 of the follow-up cases were noninvasive, and the remaining GGO with a solid component was judged to be minimally invasive adenocarcinoma because the size of the collapse fibrosis was only 2 mm in diameter (Fig. 1F).

TABLE 2. Thin-Section CT Findings, Progression Types, and Doubling Time of Ground-Glass Opacities

Case No.	Follow-Up Phase with Thin-Section CT: GGO Size (mm) First	GGO Size (mm) Final	Final TS-CT of GGO: Density	Solid	Finding	Progression Type	Period of Follow-Up with TS-CT (Months)*	GGO Doubling Time (Days)
1	17	12	Increasing	+	Mixed	Dec	12	−214
2	14	12	Increasing	+	Mixed	Dec	37	−1680
3	6.5	7.5	Stable	−	Pure	Inc	13	617
4	7	10.5	Stable	−	Pure	Inc	22	383
5	7	7	Increasing	−	Pure	Den	27	—
6	8.5	9.5	Stable	−	Pure	Inc	12	669
7	6.5	9	Stable	−	Pure	Inc	10	216
8	13.5	16.5	Stable	−	Pure	Inc	6	198

CT, computed tomography; GGO, ground-glass opacity; TS-CT, thin-section computed tomography; Inc, increasing; Dec, decreasing; Den, density.
*Number of months was rounded.

© 2004 Lippincott Williams & Wilkins

TABLE 3. Evolution of Solid Components in Ground-Glass Opacities

Case No.	Follow-Up Phase with TS-CT Solid Size (mm) First TS-CT	Months After the First TS-CT 6	11	23	36	Doubling Time (Days)
1	0*	8				14*
2	0	—	2	3	7.5	130†

TS-CT, thin-section computed tomography.
*Doubling time of solid component in case 1 was calculated on the assumption that the first size was 0.5 mm.
†Doubling time of solid component in case 2 was calculated based on the sizes between 11 months and 36 months after the first TS-CT.

Doubling Time

The doubling times of the increasing-type opacities ranged from 198 to 669 days (mean ± SD, 417 ± 220 days). The doubling time of the density-type opacity could not be calculated because it did not change in size. For the decreasing-type opacities, the doubling times were calculated based on the sizes of the pGGOs and the solid components, individually. In case 1, the doubling times of the pGGO and the solid component were −214 and 14 days, respectively. In case 2, the doubling times of the pGGO and the solid component were 1680 and 130 days, respectively.

Correlation of Thin-Section CT Images and Pathologic Findings

The pGGO corresponded to the lepidic growth of cancer cells (Fig. 1E), the thickening of the alveolar wall (Fig. 1E), and the collapse of the alveolar space (Fig. 1E). Solid components corresponded not only to the collapse of the alveolar space and fibrosis (Fig. 1F and Fig. 2G), but also to a severe narrowing of the alveolar space (Fig. 1F). With the development of a solid component in case 2, the distance between the surrounding pulmonary veins and the bronchus gradually narrowed (Figs. 2C–F). The same finding was observed in case 1 (Figs. 1C, D).

DISCUSSION

To our knowledge, this study is the first report to describe the progression of pGGOs in minute lung cancers that appeared as new pGGOs during the screening process or arose from inconspicuous minute nodules on low-dose helical CT screening images obtained at 6-month intervals. In addition, the progressions of the pGGOs on the thin-section CT images were classified into 3 types for the first time. Although a few papers have described the natural history of GGOs in pulmonary adenocarcinoma,[4,7,12,15–17] only 1 researcher[15] reported 2 GGOs that decreased in size, but the size reduction occurred in mixed GGOs, not in pGGOs. The rapid decreasing of a pGGO and the appearance of a solid component has not previously been reported.

Radiologic-pathologic correlations revealed that pGGOs on thin-section CT images mainly represent the lepidic growth of adenocarcinomas.[1,3,4,12,15–17] Solid components in the mixed GGOs were caused by the collapse of alveolar spaces or regions of fibrosis[12] and by a severe narrowing of the alveolar space (case 1). The narrowing of the distance between the surrounding pulmonary vessels and the bronchus was caused not only by the collapse of the alveolar space (cases 1 and 2), but also by the development of fibrosis (case 1) in the pGGO lesions. This finding has been termed "vessel convergence."[12,15,17] Based on our observations of the progression from a pure GGO to a mixed GGO in cases 1 and 2, our results also support the stepwise progression of replacement-type adenocarcinoma.[12,15,17]

Although 1 researcher raised serious questions about the concept of 2-year stability implying benignity,[25] pulmonary nodules are generally considered to be benign if they remain the same size or decrease in size over a 2-year observation period.[26,27] However, our results show that stability or reduction in size over a 2-year period does not necessarily indicate benignity. In the case of a pGGO that decreases in size, can the Schwartz equation be applied to a change from a pGGO to a mixed GGO if the area of the GGO decreases? Usually, the Schwartz equation is based on the assumption that constant exponential tumor growth is the basic pattern of neoplastic proliferation.[22] The doubling time for mixed GGOs has been reported to be 457 ± 260 days.[28] However, progression to a mixed GGO in a case where the pGGO decreases in size and a solid component simultaneously appears has not previously been reported. Moreover, the calculation of doubling times for each component in a mixed GGO has never, to the best of our knowledge, been performed prior to the current study. The doubling time for the solid component in case 1 was calculated based on the assumption that the initial size of the solid component was 0.5 mm, this because the thin-section CT images were taken not only by the single-slice CT scanner described above, but by a multislice CT scanner with the imaging parameters set at 0.5 mm × 4 rows and image reconstruction performed at 1-mm intervals.

Whether pGGOs should be resected or followed up is controversial. Definite evidence of the natural history of pGGOs does not exist at present. However, based on the indirect corroboration described below, we suggest that close follow-up until the appearance of a solid component may be a valid option for the management of pGGO. First, most pGGOs are either atypical adenomatous hyperplasia (preinvasive lesions according to the 1999 WHO criteria), BAC (a noninvasive lesion), or minimally invasive adenocarcinoma.[1,8,29] Second, 1 researcher[7] has previously reported information concerning

© 2004 Lippincott Williams & Wilkins

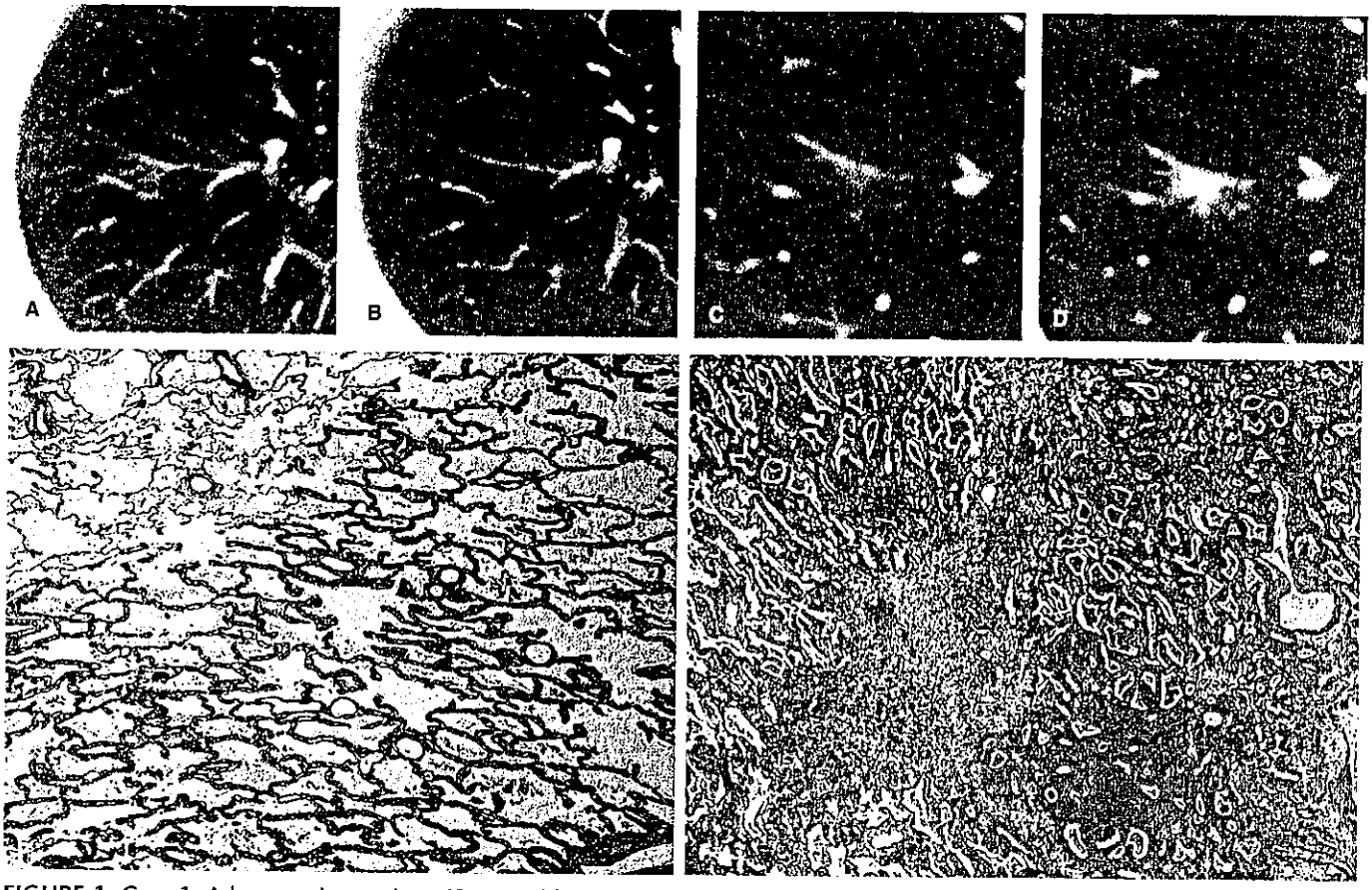

FIGURE 1. Case 1: Adenocarcinoma in a 69-year-old man. A, A faint localized increase in density was identified in segment 1 of the right upper lobe of the lung on a CT screening image obtained in December 2001. B, In retrospect, the opacity was also present on a CT screening image obtained in June 1998. C, Thin-section CT image obtained in December 2001 showing a pGGO in segment 1 of the right upper lobe of the lung. D, Thin-section CT image obtained in June 2002 shows a decrease in the size of the pGGO and the appearance of a solid component. E, Medium-magnification image of the pathologic specimen (H&E staining, ×40). Thickening of the alveolar walls as a result of the tumor cells is visible. F, Medium-magnification image of the pathologic specimen (H&E staining, ×40). Severe narrowing of the alveolar space from the thickening of the alveolar walls and an area of collapse-fibrosis with active fibroblastic proliferation are visible. A right upper lobectomy was performed in January 2003. The lesion was diagnosed as an adenocarcinoma, 17 mm in diameter (Noguchi type C). The size of collapse- fibrosis was 2 mm in diameter.

the natural history of pGGOs after conducting a long-term follow-up study lasting more than 2 years. Five of the 19 cases of pGGOs were diagnosed as lung cancers, that is, 5 BACs (1 case had 2 BACs) and 1 adenocarcinoma, after a mean follow-up of 61 months. Although the patient with adenocarcinoma was followed up for 124 months, personal communication with the author revealed that his lung cancer was of pathologic stage IA and that the size of the central fibrosis of the adenocarcinoma was less than 3 mm in diameter. We have also experienced 2 other pGGOs that developed into mixed GGOs after a 1-year and a 3-year follow-up period, respectively (unpublished data). These lesions were diagnosed as pathologic stage IA adenocarcinomas, and the size of the central fibrosis was 1.5 mm and 2 mm in diameter, respectively. Regarding the relationship between central fibrosis and prognosis, our research team[30] previously reported that 21 out of 100 patients with a lung adenocarcinoma that was 3 cm or less in diameter and which had a central fibrosis of 5 mm or less in diameter had a 5-year survival rate of 100%. Therefore, the adenocarcinoma follow-up cases described above and in this study were thought to be minimally invasive, allowing the possibility of a cure. Third, the adenocarcinoma cases with mixed GGOs did not experience any relapses or deaths, even though the solid components of the GGOs became larger but remained less than 50% of the mixed GGO nodule, this from the standpoint of the GGO's length,[31] the vanishing ratio of GGO[10] ("air-containing type"), and the volume of the GGO.[9] Finally, adenocarcinoma pGGOs tend to grow slowly, as the mean doubling time of pGGOs has been reported to be 813 days[28] or 880 days.[12] In addition, one-fourth of the GGOs in 1 study were

© 2004 Lippincott Williams & Wilkins

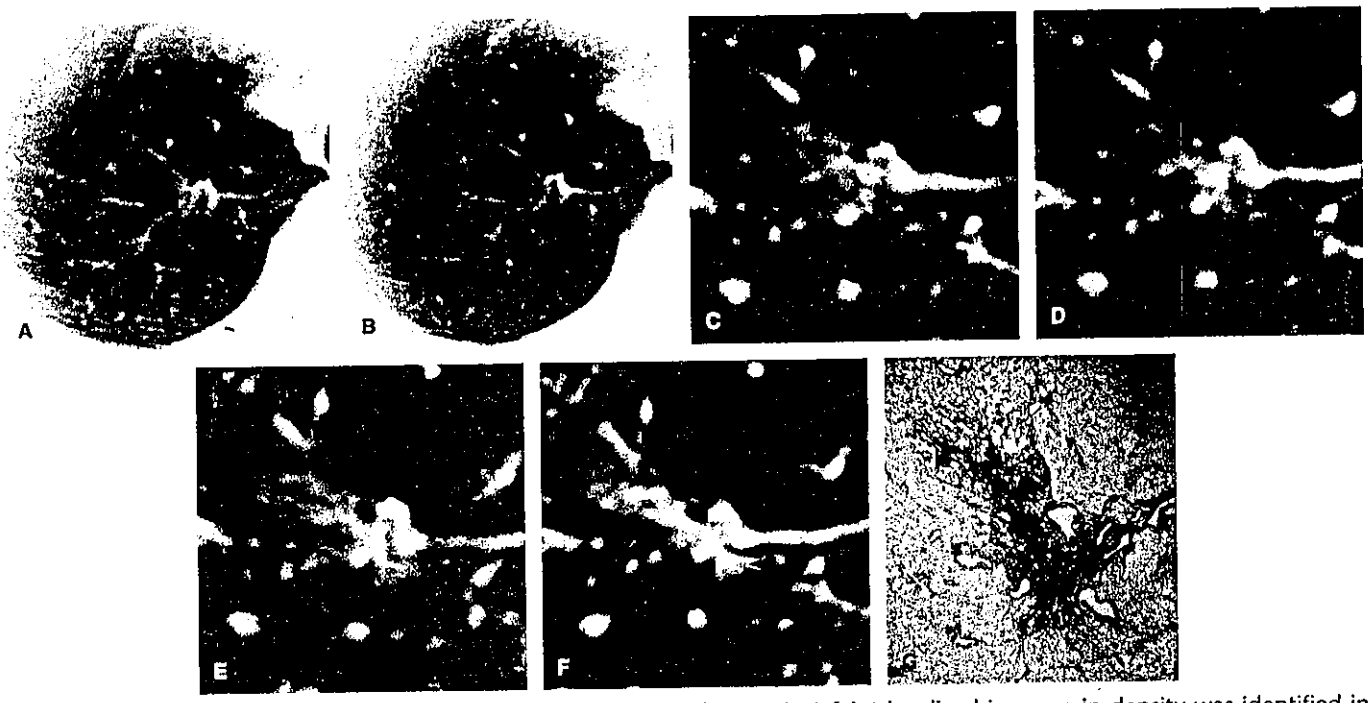

FIGURE 2. Case 2: Bronchioloalveolar carcinoma in a 69-year-old man. A, A faint localized increase in density was identified in segment 1 of the right upper lobe of the lung on a CT screening image obtained in February 1999. B, In retrospect, the opacity was also visible on a CT screening image obtained in February 1998. C, Thin-section CT revealed a pGGO in segment 1 of the right upper lobe of the lung in March 1999. D, Thin-section CT image obtained in February 2000 showing a pGGO with a small solid component. E, Thin-section CT image obtained in February 2001 showing a decrease in the size of the pGGO and a slight increase in the size of the solid component. F, Thin-section CT image obtained in February 2002 showing a larger decrease in the size of the pGGO and an increase in the size of the solid component. G, Low-magnification image of the pathologic specimen (H&E staining, ×5). The foci of alveolar collapse (asterisks) are shown. A right upper lobectomy was performed in May 2002. The lesion was diagnosed as a bronchioloalveolar carcinoma, 15 mm in diameter (Noguchi type B).

stable after a mean follow-up period of 16 months,[17] whereas half of the pGGOs in another study showed no change in size after a median follow-up period of 32 months.[7] Therefore, the classification of some pGGOs may be affected by an overdiagnosis bias.

This study has some limitations. First, the period of pGGO development was not accurately assessed because only thick-sectioned screening CT images were available for the unidentified phase. Therefore, the partial volume effect affected the detectability of small faint opacities on screening CT images. Multislice CT imaging using a narrow collimation and thinner reconstruction images may reveal the natural history of pGGOs more precisely. Second, measurements made with a pair of calipers to calculate doubling times may lead to measurement errors. Although technical advances have been reported,[32,33] we did not have any commercial software for volume measurements. Third, our study cohort was very small. At the start of the helical CT screening project, surgery without follow-up tended to be recommended in cases with pGGO. After knowledge of pGGOs had accumulated (ie, that most pGGOs consisted of preinvasive, noninvasive, or minimally invasive lesions), our treatment procedure changed.[8] Now, resection is only 1 option, not the only option, as in the past. Because of this, resection data cannot always be obtained, and the number of cases was small as a result.

In conclusion, the natural history of pGGOs detected by helical CT screening for lung cancer was partially revealed. A classification for pGGO progression was proposed based on thin-section CT images obtained during the follow-up phase. The pGGOs of lung cancer nodules do not only increase in size or density, but may also decrease rapidly or slowly with the appearance of solid components. Close follow-up until the appearance of a solid component may be a valid option for the management of pGGO.

ACKNOWLEDGMENTS

The authors thank Fumio Shishido, MD, PhD (Department of Radiology, School of Medicine, Fukushima Medical University) for his encouragement. We also wish to thank the pathologists who assisted in this study: Yoshihiro Matsuno, MD (National Cancer Center Research Institute), Tomoyuki Yokose, MD, and Genichiro Ishii, MD (National Cancer Center Research Institute East). We also thank the physicians, the

© 2004 Lippincott Williams & Wilkins

technical staff, and the administrative staff of the Anti–Lung Cancer Association in Tokyo.

REFERENCES

1. Nakajima R, Yokose T, Kakinuma R, et al. Localized pure ground-glass opacity on high-resolution CT: histologic characteristics. *J Comput Assist Tomogr*. 2002;26:323–329.
2. Nakata M, Saeki H, Takata I, et al. Focal ground-glass opacity detected by low-dose helical CT. *Chest*. 2002;121:1464–1467.
3. Kuriyama K, Seto M, Kasugai T, et al. Ground-glass opacity on thin-section CT: value in differentiating subtypes of adenocarcinoma of the lung. *AJR Am J Roentgenol*. 1999;173:465–469.
4. Yang ZG, Sone S, Takashima S, et al. High-resolution CT analysis of small peripheral lung adenocarcinomas revealed on screening helical CT. *AJR Am J Roentgenol*. 2001;176:1399–1407.
5. Henschke CI, Yankelevitz DF, Mirtcheva R, et al. CT screening for lung cancer: frequency and significance of part-solid and nonsolid nodules. *AJR Am J Roentgenol*. 2002;178:1053–1057.
6. Kodama K, Higashiyama M, Yokouchi H, et al. Prognostic value of ground-glass opacity found in small lung adenocarcinoma on high-resolution CT scanning. *Lung Cancer*. 2001;33:17–25.
7. Kodama K, Higashiyama M, Yokouchi H, et al. Natural history of pure ground-glass opacity after long-term follow-up of more than 2 years. *Ann Thorac Surg*. 2002;73:386–393.
8. Suzuki K, Asamura H, Kusumoto M, et al. "Early" peripheral lung cancer: prognostic significance of ground-glass opacity on thin-section computed tomographic scan. *Ann Thorac Surg*. 2002;74:1635–1639.
9. Matsuguma H, Yokoi K, Anraku M, et al. Proportion of ground-glass opacity on high-resolution computed tomography in clinical T1N0M0 adenocarcinoma of the lung: a predictor of lymph node metastasis. *J Thorac Cardiovasc Surg*. 2002;124:278–284.
10. Kondo T, Yamada K, Noda K, et al. Radiologic-prognostic correlation in patients with small pulmonary adenocarcinomas. *Lung Cancer*. 2002;36:49–57.
11. Austin JM, Muller NL, Friedman PJ, et al. Glossary of terms for CT of the lung: recommendations of the Nomenclature Committee of the Fleischner Society. *Radiology*. 1996;200:327–331.
12. Aoki T, Nakata H, Watanabe H, et al. Evolution of peripheral lung adenocarcinomas: CT findings correlated with histology and tumor doubling time. *AJR Am J Roentgenol*. 2000;174:763–768.
13. White CS, Romney BM, Mason AC, et al. Primary carcinoma of the lung overlooked at CT: analysis of findings in 14 patients. *Radiology*. 1996;199:109–115.
14. Gurney JW. Missed lung cancer at CT: imaging findings in nine patients. *Radiology*. 1996;199:117–122.
15. Koizumi N, Sakai K, Matsuzuki Y, et al. Natural history of cloudy zone of pulmonary adenocarcinoma on HRCT [in Japanese]. *Nippon Igaku Hoshasen Gakkai Zasshi*. 1996;56:715–719.
16. Jang HJ, Lee KS, Kwon OJ, et al. Bronchioloalveolar carcinoma: focal area of ground-glass attenuation at thin-section CT as an early sign. *Radiology*. 1996;199:485–488.
17. Takashima S, Maruyama Y, Hasegawa M, et al. CT findings and progression of small peripheral lung neoplasms having a replacement growth pattern. *AJR Am J Roentgenol*. 2003;180:817–826.
18. Kakinuma R, Ohmatsu H, Kaneko M, et al. Detection failures in spiral CT screening for lung cancer: analysis of CT findings. *Radiology*. 1999;212:61–66.
19. Li F, Sone S, Abe H, et al. Lung cancers missed at low-dose helical CT screening in a general population: comparison of clinical, histopathologic, and imaging findings. *Radiology*. 2002;225:673–683.
20. Kaneko M, Eguchi K, Ohmatsu H, et al. Peripheral lung cancer: screening and detection with low-dose spiral CT versus radiography. *Radiology*. 1996;201:798–802.
21. Sobue T, Moriyama N, Kaneko M, et al. Screening for lung cancer with low-dose helical computed tomography: Anti–Lung Cancer Association project. *J Clin Oncol*. 2002;20:911–920.
22. Schwartz M. A biomathematical approach to clinical tumor growth. *Cancer*. 1961;14:1272–1294.
23. Travis W, Colby T, Corrin B, et al. *Histological Typing of Lung and Pleural Tumors*. Berlin: Springer; 1999.
24. Noguchi M, Morikawa A, Kawasaki M, et al. Small adenocarcinoma of the lung: histologic characteristics and prognosis. *Cancer*. 1995;75:2844–2852.
25. Yankelevitz DF, Henschke CI. Does 2-year stability imply that pulmonary nodules are benign? *AJR Am J Roentgenol*. 1997;168:325–328.
26. Swensen SJ, Jett JR, Hartman TE, et al. Lung cancer screening with CT: Mayo Clinic experience. *Radiology*. 2003;226:756–761.
27. Benjamin MS, Drucker EA, McLoud TC, et al. Small pulmonary nodules: detection at chest CT and outcome. *Radiology*. 2003;226:489–493.
28. Hasegawa M, Sone S, Takashima S, et al. Growth rate of small lung cancers detected on mass CT screening. *Br J Radiol*. 2000;73:1252–1259.
29. Nakata M, Sawada S, Saeki H, et al. Prospective study of thoracoscopic limited resection for ground-glass opacity selected by computed tomography. *Ann Thorac Surg*. 2003;75:1601–1606.
30. Suzuki K, Yokose T, Yoshida J, et al. Prognostic significance of the size of central fibrosis in peripheral adenocarcinoma of the lung. *Ann Thorac Surg*. 2000;69:893–897.
31. Aoki T, Tomoda Y, Watanabe H, et al. Peripheral lung adenocarcinoma: correlation of thin-section CT findings with histologic prognostic factors and survival. *Radiology*. 2001;220:803–809.
32. Yankelevitz Df, Reeves AP, Kostis WJ, et al. Small pulmonary nodules: volumetrically determined growth rates based on CT evaluation. *Radiology*. 2000;217:251–256.
33. Ko JP, Rusinek H, Jacobs EL, et al. Small pulmonary nodules: volume measurement at chest CT-phantom study. *Radiology*. 2003;228:864–870.

© 2004 Lippincott Williams & Wilkins

ELSEVIER

European Journal of Cardio-thoracic Surgery 25 (2004) 877–883

EUROPEAN JOURNAL OF CARDIO-THORACIC SURGERY

www.elsevier.com/locate/ejcts

Prognosis and histologic features of small pulmonary adenocarcinoma based on serum carcinoembryonic antigen level and computed tomographic findings

Kazuya Takamochi[a,*], Junji Yoshida[b], Mitsuyo Nishimura[b], Tomoyuki Yokose[c], Satoshi Sasaki[d], Yutaka Nishiwaki[b], Kazuya Suzuki[a], Kanji Nagai[b]

[a]*First Department of Surgery, Hamamatsu University School of Medicine, 1-20-1 Handayama, Shizuoka, Hamamatsu 431-3192, Japan*
[b]*Division of Thoracic Oncology, National Cancer Center Hospital East, Chiba, Japan*
[c]*Pathology Division, National Cancer Center Research Institute East, Chiba, Japan*
[d]*National Institute of Health and Nutrition, Tokyo, Japan*

Received 8 November 2003; received in revised form 21 January 2004; accepted 28 January 2004

Abstract

Objectives: In 2001, we proposed the criteria for combined evaluation of the serum carcinoembryonic antigen (CEA) level and the tumor shadow disappearance rate (TDR) to predict pathologic N0 (pN0) disease in pulmonary adenocarcinomas. The objective of the present study was to determine the prognosis and histologic features in small-sized pulmonary adenocarcinomas according to serum CEA level and TDR. **Methods:** We reviewed clinical records of 189 consecutive patients with peripheral pulmonary adenocarcinoma 3.0 cm or smaller who underwent major lung resection and systematic lymph node dissection: 50 patients with TDR 0.8 or more and normal CEA level (group I) and 139 patients with TDR <0.8 and/or elevated CEA level (group II). Among them, we investigated histologic features of 177 adenocarcinomas according to serum CEA level and TDR. **Results:** The 5-year survival rates were 95% for group I and 75% for group II ($P = 0.002$), and for pN0 patients, 97% in group I and 87% in group II ($P = 0.04$). In univariate analyses, TDR, preoperative serum CEA level, and the maximum tumor dimension on computed tomographic (CT) scan were significantly associated with prognosis. Multivariate analysis showed that only preoperative serum CEA level and TDR were significant independent prognostic factors, and the maximum tumor dimension was not significant. Group I patients developed no local recurrence, including lymph node metastases. In 25 group I adenocarcinomas 2.0 cm or smaller, no lymph node involvement, two lymphatic permeation, two vascular invasion, and one pleural involvement tumors were observed. These signs of local invasiveness were less frequent than the remaining adenocarcinomas. CT findings correlated well with histologic findings in small-sized adenocarcinomas. **Conclusions:** Combined evaluation of preoperative serum CEA level and TDR may enable us to identify minimally invasive adenocarcinomas with good prognosis. Candidates for limited lung resection without systematic lymph node dissection could be selected based on these findings.
© 2004 Elsevier B.V. All rights reserved.

Keywords: Lung cancer; Limited surgery; Carcinoembryonic antigen; Computerized tomography scan; Adenocarcinoma

1. Introduction

Many small-sized lung cancers, especially peripheral adenocarcinomas, have been found as a result of the introduction of computed tomographic (CT) screening for lung cancer [1]. Among them, bronchioloalveolar carcinoma (BAC) with small invasive foci has been found increasingly. Several investigators reported that these BAC type adenocarcinomas are likely to appear as localized ground glass attenuation (GGA) [2–5]. In the latest edition of World Health Organization (WHO) classification of lung tumors [6], BAC is classified as non-invasive carcinoma. If the relationship between GGA and BAC is conclusive, candidates for limited lung resection could be selected based on CT findings.

We previously reported that pathologic N0 (pN0) status in peripheral pulmonary adenocarcinoma was predictable by the combined evaluation of serum carcinoembryonic antigen (CEA) level and a radiological parameter, tumor shadow disappearance rate (TDR) [7]. TDR is the ratio of a maximum tumor area in mediastinal window setting images to that in

* Corresponding author. Tel.: +81-53-435-2276; fax: +81-53-435-2272.
E-mail address: ktakamoc@hama-med.ac.jp (K. Takamochi).

1010-7940/$ - see front matter © 2004 Elsevier B.V. All rights reserved.
doi:10.1016/j.ejcts.2004.01.049

pulmonary window setting images on conventional CT scans. We speculated that TDR could be interpreted as the extent of both GGA and BAC. However, we did not show in the previous study the data on the correlation between TDR and histologic features and prognostic implication of TDR.

The objective of the present study was to determine the prognosis and histologic features in small-sized pulmonary adenocarcinomas according to serum CEA level and TDR.

2. Patients and methods

2.1. Patients

From August 1992 to April 1997, 189 consecutive patients with peripheral adenocarcinoma 3.0 cm or smaller who underwent major lung resection and systematic lymph node dissection at the National Cancer Center Hospital East were reviewed. One hundred and eighty-five lobectomies, three lobectomies with bronchoplastic procedures, and one pneumonectomy were carried out. There were 89 men and 100 women. The mean age was 63 years, ranging from 33 to 84 years.

2.2. Outcome and patterns of failure

All clinical records were carefully reviewed to examine patterns of failure and outcome. The median follow-up period for the 189 patients was 57 months. The length of survival was defined as the interval in months between the day of surgical intervention and the date of death due to any cause or the last follow-up. The survival rates were calculated by the Kaplan–Meier method, and the curve differences were tested using the log-rank test. Because the median follow-up time was less than 5 years, we calculated 3- and 5-year survival rates separately.

As in our previous report [7], the following tumor dimensions on conventional CT scan was defined: pDmax, the maximum dimension of a tumor on pulmonary window setting images; pDperp, the largest dimension perpendicular

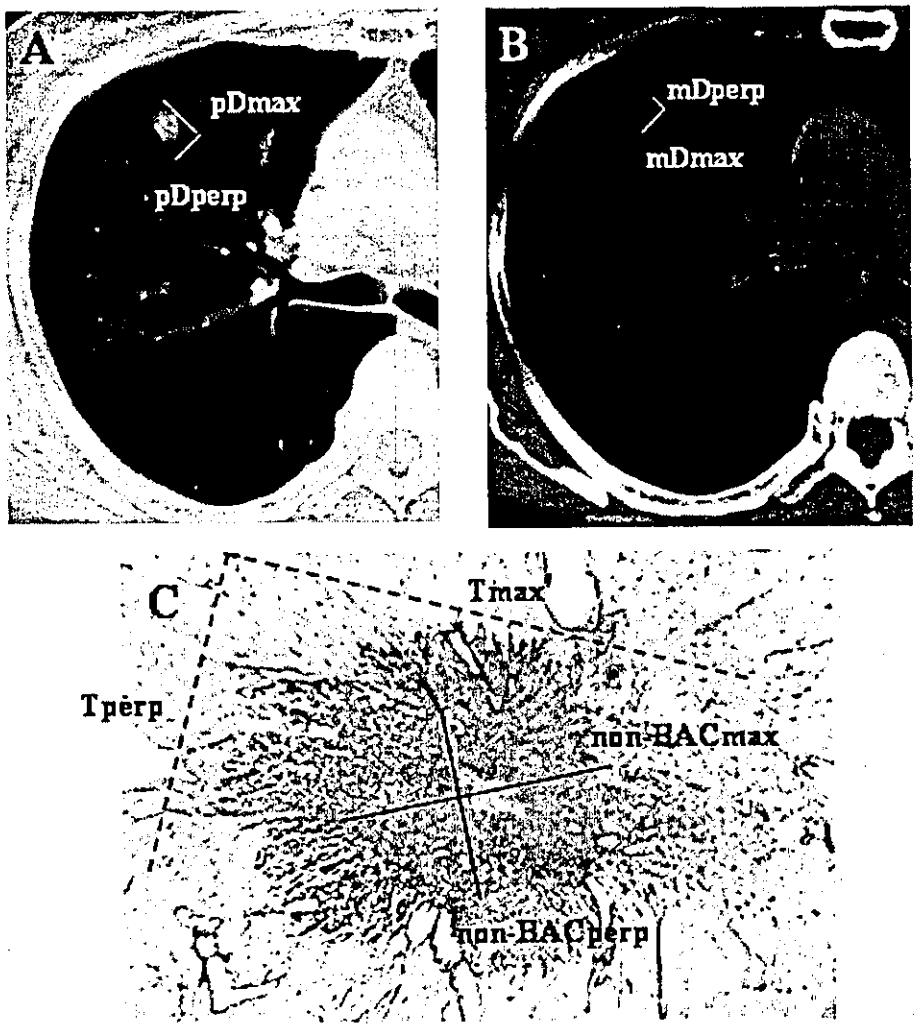

Fig. 1. We measured pDmax and pDperp on pulmonary window setting images (A), and mDmax and mDperp on mediastinal window setting images (B). We also measured Tmax, Tperp, non-BACmax, and non-BACperp at the maximum tumor dimension on low power views (hematoxylin and eosin stain, original magnification 5 ×) as illustrated (C).

to the maximum axis on pulmonary window setting images; mDmax, the maximum dimension of a tumor on mediastinal window setting images; and mDperp, the largest dimension perpendicular to the maximum axis on mediastinal window setting images (Fig. 1A and B). TDR was calculated by the following formula as previously described [7]:

$$TDR = 1 - \frac{(mDmax) \times (mDperp)}{(pDmax) \times (pDperp)}$$

Univariate and multivariate analyses were performed by means of Cox's proportional hazards model on Stat View 5.0 (Abecus Concepts, Inc., Berkeley, CA). In multivariate analysis, forward and backward stepwise procedures were used to determine the combination of preoperatively available factors that were essential in predicting prognosis. The present multivariate analysis included five variables: gender, age, TDR, preoperative serum CEA level, and pDmax. In the statistical analyses, we used continuous variables for age, pDmax, and TDR. Because the distribution of serum CEA values was positively skewed, we used the log-transformed values to normalize the distribution.

2.3. Histologic features

Two authors (K.T. and T.Y.) reviewed 177 of 189 pathologic materials of tumors to investigate histologic features. The resected specimens were fixed with 10% formalin or 99.8% methanol injected directly through the bronchial tree or pleura to be fully expanded. Because material fixation was inappropriate for histologic review, 12 cases were excluded. We studied lymphatic permeation, vascular invasion, pleural involvement, and scar grade [8]. Additionally, we measured the following tumor parameters at the maximum tumor dimension on low power view: Tmax, the maximum tumor dimension; Tperp, the largest tumor dimension perpendicular to the maximum axis; non-BACmax, the maximum dimension of a tumor component other than BAC; and non-BACperp, the largest dimension perpendicular to the maximum axis of the non-BAC component (Fig. 1C). The BAC component was defined as a component of lepidic growth patterns of tumor cells. The non-BAC component was composed of papillary, tubular, and/or solid growth pattern components, with or without fibrotic focus, collapse, necrosis, and/or mucus in a tumor. The size of the non-BAC component was evaluated microscopically on elastica van Gieson as well as standard hematoxylin and eosin staining preparations.

In order to examine the correlation between tumor measurements on CT scans and those on pathologic specimens, we calculated Pearson's correlation coefficient (r). The χ^2-test was used to compare several variables between subgroups according to serum CEA level and TDR. In all statistical analyses, differences were considered statistically significant when $P < 0.05$.

Table 1
Clinicoradiologic characteristics of patients according to TDR and serum CEA level

	TDR ≥ 0.8 and normal CEA level (group I)	TDR < 0.8 and/or elevated CEA level (group II)
No. of patients	50	139
No. of pN0 patients (%)	49 (98)	93 (67)
Age (years, mean ± SD)	64 ± 10	62 ± 10
Gender (male/female)	14/36	75/64
CEA (ng/ml) median	2.3	3.8
(25th, 75th percentile)	(1.8, 3.3)	(2.4, 7.1)
pDmax , mm (mean ± SD)	19 ± 6	23 ± 5
pDperp, mm (mean ± SD)	15 ± 5	18 ± 5
mDmax, mm (mean ± SD)	3 ± 4	16 ± 7
mDperp, mm (mean ± SD)	2 ± 2	12 ± 6
TDR (mean ± SD)	0.96 ± 0.05	0.55 ± 0.22

3. Results

3.1. Patients

The clinical characteristics of the patients are presented in Table 1. There were 49 (98%) pN0 cases and one pathologic N1 (pN1) case in the 50 peripheral adenocarcinoma patients with TDR 0.8 or more and normal preoperative serum CEA level (group I). There were 93 (67%) pN0 cases in the 139 peripheral adenocarcinoma patients with TDR <0.8 and/or elevated preoperative serum CEA level (group II).

3.2. Outcome and patterns of failure

The overall 3- and 5-year survival rates were 88 and 80%, respectively. The 3- and 5-year survival rates of group I patients were 98 and 95%, and those of group II patients were 84 and 75%, respectively. The survival curves showed a statistically significant difference between the two groups ($P = 0.002$; Fig. 2). In pN0 patients, the overall 3- and 5-year

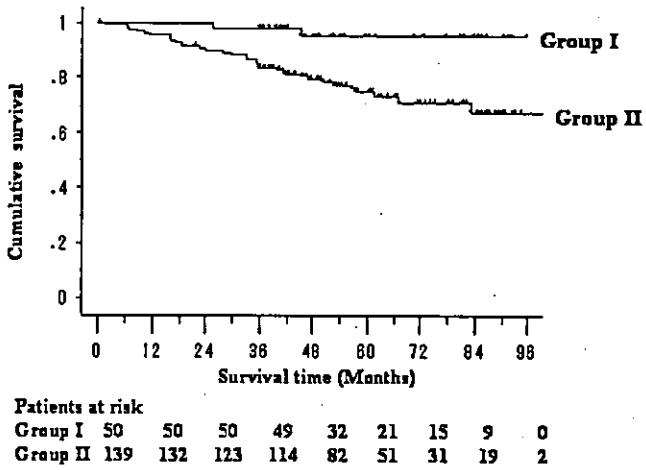

Fig. 2. Survival curves for group I and II patients. A statistically significant difference was observed between the outcomes of group I and II patients (log-rank test, $P = 0.002$).

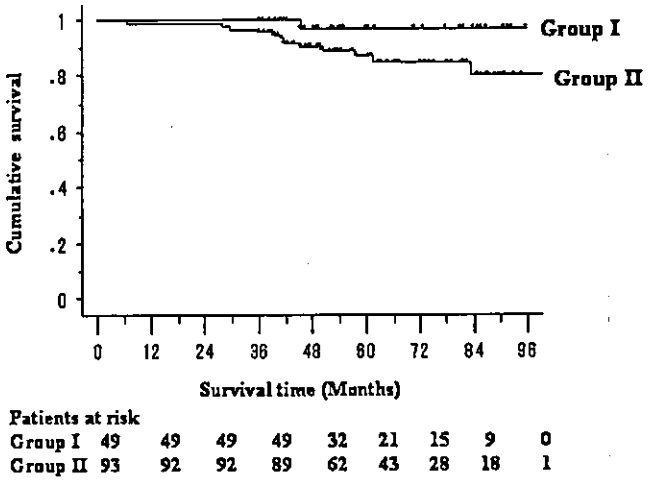

Fig. 3. Survival curves for group I and II pathologic N0 patients. A statistically significant difference was observed between the outcomes of pathologic N0 patients in groups I and II (log-rank test, $P = 0.04$).

survival rates were 97 and 91%, respectively. The 3- and 5-year survival rates of pN0 patients in group I were 100 and 97%, and those in group II were 96 and 87%, respectively. The survival curves also showed a statistically significant difference between the two groups ($P = 0.04$; Fig. 3).

Two patients in group I died during follow-up period. One developed brain and bone metastases 44 months after initial surgical resection, and died of primary lung cancer. The other was the only patient with pN1 disease and died of lower gingival cancer without any signs of primary lung cancer recurrence. No group I patients developed local recurrence including mediastinal lymph node metastases. The other 48 group I patients were alive with no signs of recurrence. Of 139 group II patients, 36 (26%) developed local and/or distant recurrences: 7 (5%) patients showed mediastinal lymph node metastases, 5 (4%) supraclavicular lymph node metastases, and 31 (22%) distant metastases (Table 2).

In univariate analyses (Table 3), TDR ($P = 0.004$), preoperative serum CEA level ($P = 0.002$), and pDmax ($P = 0.008$) were significantly associated with prognosis. In multivariate analysis, TDR ($P = 0.02$) and preoperative serum CEA level ($P = 0.03$) were shown to be independently significant prognostic factors.

Table 2
Patterns of failure in peripheral pulmonary adenocarcinoma according to TDR and serum CEA level

	TDR ≥ 0.8 and normal CEA level (group I, $n = 50$)	TDR < 0.8 and/or elevated CEA level (group II, $n = 139$)
No. of recurrence (%)	1 (2)	36 (26)
Site of recurrence (%)		
Mediastinal lymph node	0 (0)	7 (5)
Supraclavicular lymph node	0 (0)	5 (4)
Distant metastases	1 (2)	31 (22)

Table 3
Univariate analyses of prognostic factors in peripheral pulmonary adenocarcinoma

Variable	Hazard ratio	95% CI	*P*-value
Age	0.996	0.964–1.028	0.8
Gender	0.732	0.379–1.413	0.4
CEA[a]	2.231	1.346–3.696	0.002
pDmax	1.093	1.023–1.168	0.008
TDR	0.158	0.045–0.554	0.004

CI, confidence interval.
[a] Log-transformed serum CEA levels were used.

3.3. Histologic features

The relationship between tumor histologic characteristics and TDR and serum CEA level combined according to tumor size (2.0 cm or smaller versus 2.1–3.0 cm) is shown in Table 4. No lymph node involvement was found in group I tumors 2.0 cm or smaller. Although there was one pN1, no pathologic N2 cases were found in group I tumors 2.1–3.0 cm in size. There were significantly more pN0 tumors in group I than in group II. Group I tumors were more frequently negative for lymphatic permeation and vascular invasion, and there were more lower scar grade tumors (grade 1/2 versus grade 3/4) than group II tumors. Pleural involvement tended to be negative in group I tumors 2.0 cm or smaller ($P = 0.06$) and was significantly more frequently negative in group I tumors 2.1–3.0 cm in size ($P = 0.005$) compared with group II.

Statistical correlation was shown between pDmax and Tmax ($r = 0.63$, $P < 0.0001$), pDperp and Tperp ($r = 0.61$, $P < 0.0001$), mDmax and non-BACmax ($r = 0.56$, $P < 0.0001$), mDperp and non-BACperp ($r = 0.60$, $P < 0.0001$), pDmax × pDperp and Tmax × Tperp ($r = 0.62$, $P < 0.0001$), mDmax × mDperp and non-BACmax × non-BACperp ($r = 0.58$, $P < 0.0001$; Fig. 4). These findings suggested that the measurements of non-BAC component in pathologic specimens correlated well with those of tumor opacity on mediastinal window setting images.

4. Discussion

Adenocarcinoma is the most common histologic type of lung cancer, and its incidence has been increasing [9]. Many small peripheral adenocarcinomas with BAC component have, in particular, been found since helical CT scanning was introduced for lung cancer screening [1]. In the latest edition of WHO classification [6], BAC is clearly defined as an adenocarcinoma with a pure bronchioloalveolar growth pattern and no evidence of stromal, vascular or pleural invasion. Noguchi et al. [10] classified small peripheral adenocarcinomas into six subtypes (types A–F). Type A

Table 4
The relationship between tumor histologic characteristics and TDR and serum CEA level combined according to tumor size

	pDmax 0–20 mm ($n = 69$)			pDmax 21–30 mm ($n = 108$)		
	TDR ≥ 0.8 and normal CEA level (group I) (%)	TDR < 0.8 and/or elevated CEA level (group II) (%)	P^a	TDR ≥ 0.8 and normal CEA level (group I) (%)	TDR < 0.8 and/or elevated CEA level (group II) (%)	P^a
No. of tumors	25	44		21	87	
Lymph node status						
N0	25 (100)	32 (73)		20 (95)	57 (66)	
N1	0 (0)	4 (9)		1 (5)	10 (11)	
N2	0 (0)	8 (18)	0.004	0 (0)	20 (23)	0.007
Lymphatic permeation						
Negative	23 (92)	26 (59)		18 (86)	46 (53)	
Positive	2 (8)	18 (41)	0.004	3 (14)	41 (47)	0.006
Vascular invasion						
Negative	23 (92)	27 (61)		18 (86)	45 (52)	
Positive	2 (8)	17 (39)	0.006	3 (14)	42 (48)	0.005
Pleural involvement						
Negative	24 (96)	35 (80)		21 (100)	62 (71)	
Positive	1 (4)	9 (20)	0.06	0 (0)	25 (29)	0.005
Scar grade						
1 or 2	16 (64)	8 (18)		14 (67)	18 (21)	
3 or 4	9 (36)	36 (82)	0.0001	7 (33)	69 (79)	<.0001

[a] P-value in χ^2-test.

(localized BAC) and type B (localized BAC with a focus of collapsed alveolar structure) showed no lymph node metastasis, rare vascular invasion and excellent prognosis of 100% 5-year survival rate. BAC and Noguchi's types A/B could be regarded as minimally invasive, possibly in situ, adenocarcinomas.

Recently, several investigators reported that GGA on high-resolution computed tomography (HRCT) corresponded to lepidic tumor growth in the BAC component [2–5]. A greater extent of GGA in a tumor opacity on HRCT scans correlated with histopathologic lower invasiveness and better outcomes [2,11–13]. Others reported better outcomes in adenocarcinoma with a greater extent of BAC components in pathologic specimens [14,15]. Suzuki et al. [16] reported that in peripheral pulmonary adenocarcinomas 3.0 cm or smaller, a good correlation was demonstrated between the size of central fibrosis in pathologic specimens and outcome. The central fibrosis or non-BAC component in a tumor would appear as consolidation on HRCT scans [3,5].

Based on these previous findings, we can assume that histopathologically minimally invasive adenocarcinomas, possible candidates for limited surgical resection, are predictable based on CT findings: greater extent of GGA or minimal consolidation in a tumor opacity. However, no quantitative analyses comparing the size of GGA or consolidation in tumor opacities on CT scans, with the sizes of BAC or non-BAC components in pathologic specimens have been reported previously. In this study, we showed that the size of non-BAC component

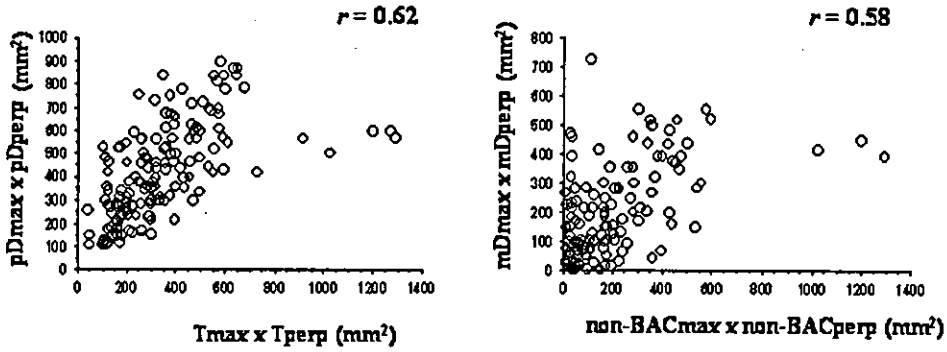

Fig. 4. Statistical correlation was shown between pDmax × pDperp and Tmax × Tperp ($r = 0.62$, $P < 0.0001$), mDmax × mDperp and non-BACmax × non-BACperp ($r = 0.58$, $P < 0.0001$).

correlated well with that of tumor opacity in mediastinal window setting images on conventional CT scans.

The most common definition of GGA is "a hazy increased attenuation of lung, but with preservation of bronchial and vascular structure" [17]. However, it is sometimes difficult to accurately define the edges of GGA when measuring its size. GGA area usually disappears in mediastinal window setting images. Measuring the size of tumor opacity in a mediastinal window-setting image is an easy and reproducible way to evaluate the size of a non-GGA area. Calculating TDR is more objective than quantifying GGA by visual estimation in a pulmonary window setting image as in previous studies [3,11,12]. However, the reproducibility and inter-observer variations in calculating TDR need to be verified in a larger prospective study. Since HRCT should yield more accurate measurements than conventional CT scans, especially in small-sized tumors, we are planning a similar study using HRCT data.

Kondo et al. [13] classified surgically resected pulmonary adenocarcinomas 2.0 cm or smaller into two types: 'air-containing type' and 'solid density type'. The air-containing type was defined as a tumor in which the tumor opacity area on a mediastinal window setting image was half or less of that on a pulmonary window setting image by visual estimation on HRCT. The solid density type, on the other hand, was defined as a tumor in which the tumor opacity area on mediastinal window setting images was more than half of that on a pulmonary window-setting image. Among 66 air-containing type adenocarcinomas, no lymph node involvement, one lymphatic permeation, one vascular invasion, and one pleural involvement tumors were observed histopathologically. The air-containing type adenocarcinoma could be considered minimally invasive. All patients with air-containing type adenocarcinomas were alive and relapse-free after a mean observation period of 851 days following resection. These results were consistent with ours. In our study, no lymph node involvement, two lymphatic permeation, two vascular invasion, and one pleural involvement tumors were observed in 25 adenocarcinomas 2.0 cm or smaller in patients with TDR 0.8 or more and normal preoperative serum CEA level. Shimosato et al. [8] initially reported prognostic impact of fibrotic focus (scar) in patients with adenocarcinomas 3.0 cm or smaller. They proposed scar grade, which correlated well with tumor invasiveness such as lymph node involvement, vascular invasion, and pleural involvement. They suggested that a small peripheral adenocarcinoma <3.0 cm with no or little collagenization (grade 1 or 2) could be considered to be in an 'early stage' of development and could be surgically curable. There were more grade 1/2 tumors in group I patients than in group II in our series. If limited lung resection is curative enough for small-sized adenocarcinomas with no or minimal invasiveness, preoperative combined evaluation of serum CEA level and TDR is useful in selecting candidates for limited lung resection.

Although a number of prognostic factors have been reported for patients with surgically resected non-small cell lung cancer, tumor size and lymph node status are considered to be the most significant prognostic factors. We showed that the outcome of group I patients was excellent (5-year survival rate: 95%) and significantly better than group II patients with completely resected adenocarcinomas 3.0 cm or smaller. Even when the prognostic impact of pathologic lymph node status was excluded, the same result was demonstrated. Multivariate analysis showed that both preoperative serum CEA level and TDR were significant independent prognostic factors. Maximum tumor dimension on CT scan was significant in univariate analysis, but not significant in multivariate analysis. These results indicate that tumor size does not have independently significant impact on prognosis in adenocarcinomas 3.0 cm or smaller.

Patients with an adenocarcinoma 2.0 cm or smaller, if preoperative serum CEA level was normal and TDR was 0.8 or more, showed no lymph node involvement (pN0) and developed no local recurrence including lymph nodes. The results suggest that limited lung resection without systematic mediastinal lymph node dissection might be acceptable for these patients. Because these factors are available preoperatively, they are useful not only to predict outcome but also to determine the extent of resection.

In summary, peripheral small-sized pulmonary adenocarcinomas predicted as pN0 by combining serum CEA level and TDR showed no mediastinal lymph node involvement and resulted in excellent outcomes without local recurrence. CT findings correlated well with histologic findings in small-sized adenocarcinomas. Signs of local invasiveness such as lymphatic permeation, vascular invasion, and pleural involvement, were rare in small-sized adenocarcinomas with normal preoperative serum CEA level and a TDR of 0.8 or more. Combined evaluation of preoperative serum CEA level and TDR may enable us to identify minimally invasive adenocarcinomas with good prognosis.

Acknowledgements

We thank Prof. J. Patrick Barron and Assistant Prof. R. Breugelmans, International Medical Communications Center, Tokyo Medical University, for reviewing the English manuscript. This study was supported in part by a Grant-in-Aid for Cancer Research from the Ministry of Health and Welfare, Japan.

References

[1] Kaneko M, Eguchi K, Ohmatsu H, Kakinuma R, Naruke T, Suemasu K, Moriyama N. Peripheral lung cancer: screening and detection with low-dose spiral CT versus radiography. Radiology 1996;201: 798–802.

[2] Aoki T, Tomoda Y, Watanabe H, Nakata H, Kasai T, Hashimoto H, Kodate M, Osaki T, Yasumoto K. Peripheral lung adenocarcinoma: correlation of thin-section CT findings with histologic prognostic factors and survival. Radiology 2001;220: 803–9.
[3] Kuriyama K, Seto M, Kasugai T, Higashiyama M, Kido S, Sawai Y, Kodama K, Kuroda C. Ground-glass opacity on thin-section CT: value in differentiating subtypes of adenocarcinoma of the lung. Am J Roentgenol 1999;173:465–9.
[4] Yang Z, Sone S, Takashima S, Li F, Honda T, Yamanda T. Small peripheral carcinomas of the lung: thin-section CT and pathologic correlation. Eur Radiol 1999;9:1819–25.
[5] Yang ZG, Sone S, Takashima S, Li F, Honda T, Maruyama Y, Hasegawa M, Kawakami S. High-resolution CT analysis of small peripheral lung adenocarcinomas revealed on screening helical CT. Am J Roentgenol 2001;176:1399–407.
[6] World Health Organization, Histological typing of lung and pleural tumours, 3rd ed. Geneva: World Health Organization; 1999.
[7] Takamochi K, Nagai K, Yoshida J, Suzuki K, Ohde Y, Nishimura M, Sasaki S, Nishiwaki Y. Pathologic N0 status in pulmonary adenocarcinoma is predictable by combining serum carcinoembryonic antigen level and computed tomographic findings. J Thorac Cardiovasc Surg 2001;122:325–30.
[8] Shimosato Y, Suzuki A, Hashimoto T, Nishiwaki Y, Kodama T, Yoneyama T, Kameya T. Prognostic implications of fibrotic focus (scar) in small peripheral lung cancers. Am J Surg Pathol 1980;4: 365–73.
[9] Barsky SH, Cameron R, Osann KE, Tomita D, Holmes EC. Rising incidence of bronchioloalveolar lung carcinoma and its unique clinicopathologic features. Cancer 1994;73:1163–70.
[10] Noguchi M, Morikawa A, Kawasaki M, Matsuno Y, Yamada T, Hirohashi S, Kondo H, Shimosato Y. Small adenocarcinoma of the lung. Histologic characteristics and prognosis. Cancer 1995;75: 2844–52.
[11] Kim EA, Johkoh T, Lee KS, Han J, Fujimoto K, Sadohara J, Yang PS, Kozuka T, Honda O, Kim S. Quantification of ground-glass opacity on high-resolution CT of small peripheral adenocarcinoma of the lung: pathologic and prognostic implications. Am J Roentgenol 2001;177: 1417–22.
[12] Kodama K, Higashiyama M, Yokouchi H, Takami K, Kuriyama K, Mano M, Nakayama T. Prognostic value of ground-glass opacity found in small lung adenocarcinoma on high-resolution CT scanning. Lung Cancer 2001;33:17–25.
[13] Kondo T, Yamada K, Noda K, Nakayama H, Kameda Y. Radiologic–prognostic correlation in patients with small pulmonary adenocarcinomas. Lung Cancer 2002;36:49–57.
[14] Koga T, Hashimoto S, Sugio K, Yoshino I, Mojtahedzadeh S, Matsuo Y, Yonemitsu Y, Sugimachi K, Sueishi K. Clinicopathological and molecular evidence indicating the independence of bronchioloalveolar components from other subtypes of human peripheral lung adenocarcinoma. Clin Cancer Res 2001;7:1730–8.
[15] Higashiyama M, Kodama K, Yokouchi H, Takami K, Mano M, Kido S, Kuriyama K. Prognostic value of bronchiolo-alveolar carcinoma component of small lung adenocarcinoma. Ann Thorac Surg 1999;68: 2069–73.
[16] Suzuki K, Yokose T, Yoshida J, Nishimura M, Takahashi K, Nagai K, Nishiwaki Y. Prognostic significance of the size of central fibrosis in peripheral adenocarcinoma of the lung. Ann Thorac Surg 2000;69: 893–7.
[17] Austin JH, Muller NL, Friedman PJ, Hansell DM, Naidich DP, Remy-Jardin M, Webb WR, Zerhouni EA. Glossary of terms for CT of the lungs: recommendations of the Nomenclature Committee of the Fleischner Society. Radiology 1996;200:327–31.

Visceral pleural invasion classification in non–small cell lung cancer: A proposal on the basis of outcome assessment

Kimihiro Shimizu, MD[a]
Junji Yoshida, MD[a]
Kanji Nagai, MD[a]
Mitsuyo Nishimura, MD[a]
Tomoyuki Yokose, MD[b]
Genichiro Ishii, MD[b]
Yutaka Nishiwaki, MD[a]

Dr Shimizu

Objective: The definition of visceral pleural invasion in lung cancer TNM classification of the International Union Against Cancer lacks detail. The purpose of this study was to evaluate the significance of the extent of pleural involvement as a prognostic factor and to propose a refined TNM classification on the basis of visceral pleural invasion.

Methods: We reviewed 1653 consecutive patients with T1, T2, and T3 surgically resected non–small cell lung cancer for their clinicopathologic characteristics and prognoses. Visceral pleural invasion was classified by using the Japan Lung Cancer Society criteria: p0, tumor with no pleural involvement beyond its elastic layer; p1, tumor extension beyond the elastic layer but no exposure on the pleural surface; and p2, tumor exposure on the pleural surface.

Results: The 5-year survivals for patients with p1 or p2 tumors of 3 cm or less were identical and significantly worse than those for patients with p0 tumors of the same size. Patients with p1 or p2 tumors of greater than 3 cm and patients with T3 cancers had essentially identical survivals.

Conclusions: Visceral pleural invasion should be defined as tumor extension beyond the elastic layer of the visceral pleura, regardless of its exposure on the pleural surface. A tumor of 3 cm or less with visceral pleural invasion should remain classified as a T2 tumor, as presently occurs in the International Union Against Cancer staging system, and tumors of greater than 3 cm with visceral pleural invasion should be upgraded to T3 status in the International Union Against Cancer TNM classification.

From the Division of Thoracic Oncology[a] and the Pathology Division,[b] National Cancer Center Research Institute East, Kashiwa, Chiba, Japan.

Supported in part by a Grant-in-Aid for cancer research from the Ministry of Health, Labour and Welfare, Japan.

Received for publication Aug 15, 2003; revisions received Oct 13, 2003; accepted for publication Nov 4, 2003.

Address for reprints: Kimihiro Shimizu, MD, PhD, Second Department of Surgery, Gunma University Faculty of Medicine, 3-39-15, Showa-machi, Maebashi, Gunma 371-8511, Japan (E-mail: kmshimiz@showa.gunma-u.ac.jp).

J Thorac Cardiovasc Surg 2004;127:1574-8

0022-5223/$30.00

Copyright © 2004 by The American Association for Thoracic Surgery

doi:10.1016/j.jtcvs.2003.11.017

Lung cancer pleural invasion was recognized as a poor prognostic factor as early as 1958 by Brewer and colleagues.[1] Visceral pleural invasion (VPI) was adopted as a specific description in the TNM classification of the International Union Against Cancer (UICC) staging system in the mid-1970s[2] and has remained unchanged until today: a tumor of any size that invades the visceral pleura is classified as T2. Although a tumor of 3 cm or less is upgraded to T2, a tumor of greater than 3 cm remains T2 in this system if a tumor has VPI.

The UICC TNM classification describes little on VPI definition. The Japan Lung Cancer Society (JLCS) classifies VPI as follows: p0, tumor with no pleural involvement beyond its elastic layer; p1, tumor that extends beyond the elastic layer of the visceral pleura but is not exposed on the pleural surface; p2, tumor that is exposed

TABLE 1. Patient characteristics

Characteristics	No. of patients (%)				
	p0	p1	p2	T3	Total
Age (y)					
Mean ± SD	64 ± 10	66 ± 9	63 ± 10	63 ± 10	63 ± 10
Range	30-85	42-89	35-85	34-83	30-89
Sex (male/female)	662/393	177/94	34/47	212/34	1085/568
Type of operation					
Segmentectomy	21 (2)	5 (2)	0 (0)	3 (1)	29 (2)
Lobectomy	993 (94)	254 (94)	79 (98)	186 (76)	1512 (91)
Pneumonectomy	41 (4)	12 (4)	2 (3)	57 (23)	112 (7)
Histology					
Adenocarcinoma	679 (64)	163 (60)	70 (87)	85 (35)	997 (60)
Squamous cell carcinoma	311 (30)	75 (28)	9 (11)	118 (48)	513 (31)
Large cell carcinoma	36 (3)	20 (7)	2 (3)	21 (9)	79 (5)
Adenosquamous carcinoma	29 (3)	13 (5)	0 (0)	22 (9)	42 (4)
Size					
≤3cm	624 (59)	107 (40)	33 (41)	38 (15)	802 (49)
>3cm	431 (41)	164 (60)	48 (59)	208 (85)	851 (51)
Pathologic					
n0	795 (75)	163 (60)	44 (54)	110 (45)	1112 (67)
n1	134 (13)	46 (17)	9 (11)	62 (25)	251 (15)
n2	126 (12)	62 (23)	28 (35)	74 (30)	290 (18)
Total	1055	271	81	246	1653

Numbers in parentheses are percentages. *n0,* No regional lymph node metastasis; *n1,* metastasis to ipsilateral peribronchial hilar lymph nodes, ipsilateral hilar lymph nodes, or both, and intrapulmonary nodes, including involvement by direct extension of the primary tumor; *n2,* metastasis to ipsilateral mediastinal lymph nodes, subcarinal lymph nodes, or both.

on the pleural surface but does not involve adjacent anatomic structures; and p3, tumor that involves adjacent anatomic structures.[3] The Society classifies a p2 tumor of any size as T2 and a p1 tumor of 3 cm or less as T1. The UICC TNM classification does not clarify whether VPI includes p1. Given that p1 pleural involvement is interpreted as VPI in the UICC classification, there appears to be an inconsistency in the T1/T2 definition between the UICC and JLCS TNM classifications. To the best of our knowledge, there have been no studies reported on p1 pleural involvement as a prognostic factor.

The purpose of this study was to evaluate the significance of p1 pleural involvement as a prognostic factor and to propose a refined TNM classification on the basis of VPI.

Patients and Methods

From February 1979 through March 2001, 1653 consecutive patients with T1, T2, or T3 non–small cell lung cancer underwent pulmonary resection (segmentectomy or more) and systematic mediastinal lymph node dissection at our institution, as described previously.[4] All these patients had curative resection, which was defined as complete removal of ipsilateral hilar and mediastinal lymph nodes together with the primary tumor. Patients who had induction chemotherapy or radiotherapy and patients with evidence of residual tumor at the surgical margin, malignant effusion, satellite lesion, or distant metastasis verified intraoperatively or by means of postoperative pathologic examination were excluded from this study. Patients were pathologically staged on the basis of the UICC TNM classification.[2] Patient characteristics are shown in Table 1.

Histopathologic studies were done according to the World Health Organization criteria,[5] and VPI was reviewed in detail. Tumor sections were stained with hematoxylin and eosin and Victoria-blue van Gieson stains. VPI was classified according to the JLCS criteria[3]: p0, tumor with no pleural involvement beyond its elastic layer; p1, tumor that extends beyond the elastic layer of the visceral pleura but is not exposed on the pleural surface (Figure 1, *A*); and p2, tumor that is exposed on the pleural surface but does not involve adjacent anatomic structures (Figure 1, *B*). All patients were divided into 7 groups, A to G, according to the tumor diameter (≤3 cm or >3 cm), VPI (p0, p1, or p2), and T3 factor, as shown in Table 2.

We analyzed the overall survival of patient groups A to G. We also evaluated survival of patients without lymph node involvement (n0) in each group. Survival was estimated by using the Kaplan-Meier method,[6] and differences in survival were determined by means of log-rank analysis.[7] Zero time was the date of pulmonary resection, and the terminal event was defined as any death.

Results

Patient Characteristics and VPI

Table 1 shows the patient characteristics. There were 568 women and 1085 men aged 30 to 89 years (mean, 63 years; median, 65 years). Extents of pulmonary resection were pneumonectomy (n = 112), lobectomy (n = 1512), and

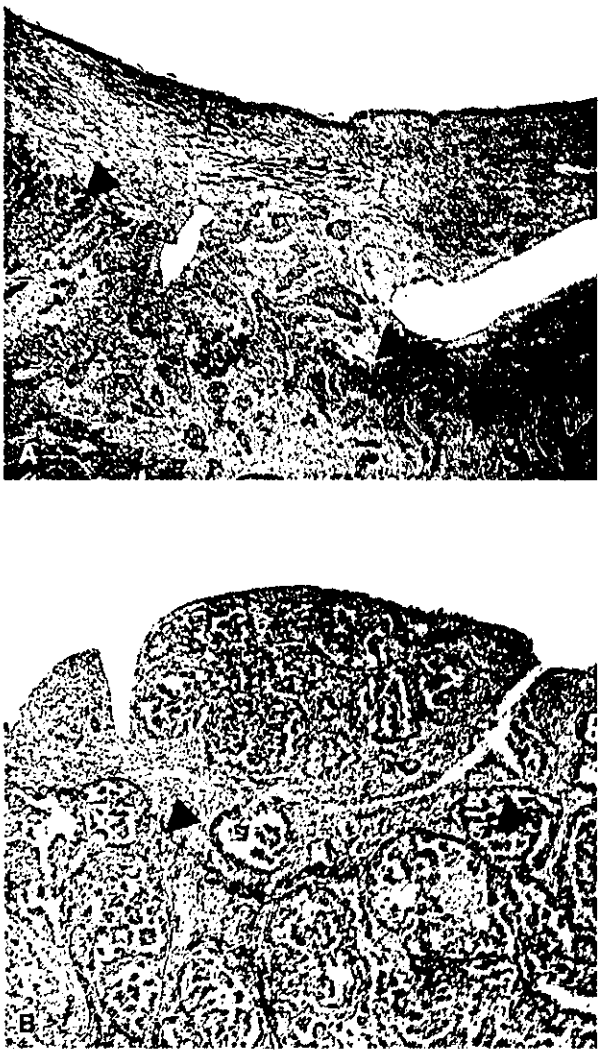

Figure 1. A, Tumor cells extend beyond the visceral pleural elastic layer *(arrowheads)* but are not exposed on the pleural surface: p1. B, Tumor cells extend beyond the visceral pleural elastic layer *(arrowheads)* and are exposed on the pleural surface but do not involve the parietal pleura: p2.

segmentectomy (n = 29). Histologic types were adenocarcinoma (n = 997), squamous cell carcinoma (n = 513), large cell carcinoma (n = 79), and adenosquamous carcinoma (n = 64).

Survival Difference

The overall 5-year survivals for groups A through G were 79%, 63%, 42%, 60%, 39%, 35%, and 36%, respectively (Figures 2 and 3). The difference in survival between groups A and B, between groups A and C, between groups B and G, and between groups C and G (Figure 2) and the difference in survival between groups D and E and between groups D and F (Figure 3) were significant. In contrast, the survival curves for groups B and D almost overlapped with each other, and there was no statistically significant difference in survival between the groups (Figure 2). Similarly, there was no statistically significant difference in survival between groups C and D and between groups B and C (Figure 2), nor was there a significant difference in survival between groups E and F (Figure 3). Also, the differences in survival between groups E and G and between groups F and G were not significant (Figure 3). Outcomes were also examined in the n0 patient cohort, and similar relationships were observed.

TABLE 2. Seven groups according to tumor diameter, VPI, and T3 factor

Group	Tumor size diameter	VPI p-factor*	All patients, n (%)	Patients with n0 disease, n (%)
A	≤3cm	p0	624 (38)	507 (46)
B	≤3cm	p1	107 (7)	79 (7)
C	≤3cm	p2	33 (2)	23 (2)
D	>3cm	p0	431 (26)	288 (26)
E	>3cm	p1	164 (10)	84 (8)
F	>3cm	p2	48 (3)	21 (2)
G	Patients with T3 tumors as defined by the UICC TNM classification		246 (15)	110 (10)

VPI, Visceral pleural invasion; *UICC*, International Union Against Cancer.
*The Japan Lung Cancer Society classification of visceral pleura invasion.

Discussion

The JLCS classifies VPI into 4 groups (p0, p1, p2, and p3), whereas in the UICC classification p1 and p2 involvements are not distinguished. If p1 pleural involvement is interpreted as VPI in the UICC classification, there appears to be inconsistency in the T1/T2 definition between the UICC and JLCS TNM classification.

Brewer and colleagues,[1] Ichinose and coworkers,[8] and Manac'h and associates[9] demonstrated that pleural invasion is an important poor prognosis factor. In their reports, however, p1 and p2 invasions were combined and analyzed as a single VPI category. In our study we conducted uniform hematoxylin and eosin and Victoria-blue van Gieson staining on all tumors and performed histologic review in all cases, with special interest in VPI and its JLCS subclassifications, p0, p1, and p2. We retrospectively analyzed postoperative survival in patients with p0, p1, p2, or T3 cancer to evaluate the significance of pleural involvement extent as a prognostic factor.

In our series the 5-year survivals for the patients with p1 or p2 tumors of 3 cm or less were identical and significantly worse than those for patients with p0 disease with the same

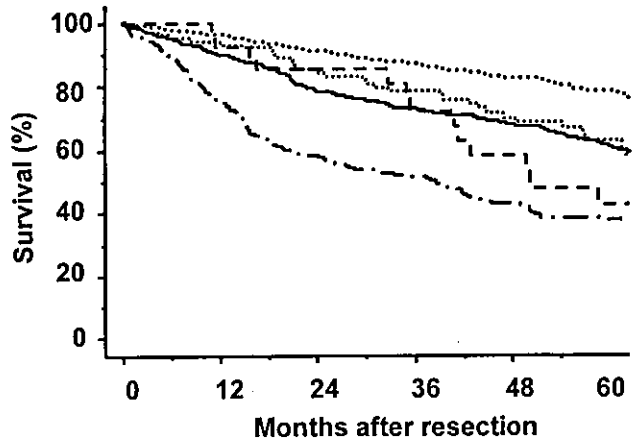

		patients (n)	5- year survival (%)	p-value*
group A	····· : ≦3cm and p0	624	79	<0.01
group B	····· : ≦3cm and p1	107	63	0.20
group C	- - - : ≦3cm and p2	33	42	0.82
group D	——— : >3cm and p0	431	60	<0.01
group G	—·-- : pT3	246	36	

*: *p*-value by log-rank test

Figure 2. Survival curves and overall 5-year survivals for groups A, B, C, D, and G. The differences in survival between groups A and B, between groups A and C ($P < .01$), between groups B and G ($P < .01$), between groups C and G ($P = .04$), and between groups D and G were significant. There was no statistically significant difference in survival between groups B and C, between groups B and D ($P = .38$), and between groups C and D.

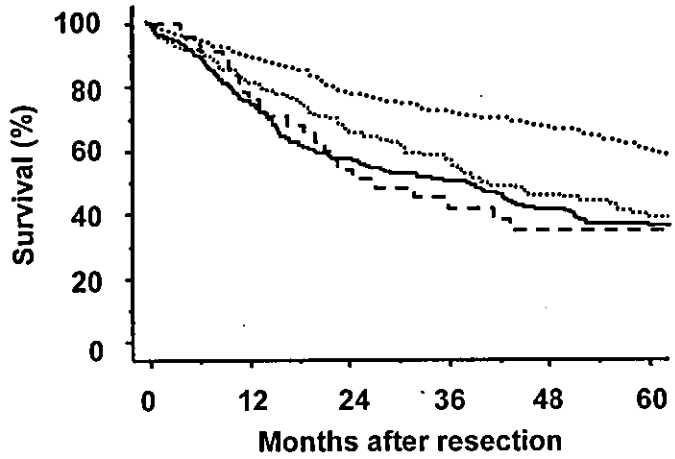

		patients (n)	5-year survival (%)	p-value*
group D	..... : >3cm and p0	431	60	<0.01
group E	..... : >3cm and p1	164	39	0.47
group F	- - - : >3cm and p2	48	35	0.90
group G	——— : pT3	246	36	

*: *p*-value by log-rank test

Figure 3. Survival curves and overall 5-year survivals for groups D, E, F, and G. The differences in survival between groups D and E, between groups D and F ($P < .01$), and between groups D and G ($P < .01$) were significant. There was no statistically significant difference in survival between groups E and F, between groups E and G ($P = .38$), and between groups F and G.

TABLE 3. Difference between the UICC, the JLCS, and our proposed new classifications

Classification	≤3 cm without VPI	≤3 cm with VPI	>3 cm without VPI	>3 cm with VPI
UICC	T1	T2	T2	T2
JLCS	T1 (p0*)	T1 (p1*) T2 (p2*)	T2 (p0*)	T2 (p1/p2*)
Ours	T1	T2	T2	T3

UICC, International Union Against Cancer; *JLCS,* Japan Lung Cancer Society; *VPI,* visceral pleura invasion.
*The Japan Lung Cancer Society classification of visceral pleura invasion.

size cancers. Similarly, the 5-year survivals for patients with p1 or p2 tumors greater than 3 cm were identical, whereas they were notably worse than those in patients with p0 disease with the same size cancers. Furthermore, there was no statistically significant difference in survival between the patients with p1 or p2 tumors greater than 3 cm and the patients with T3 cancers. Similar relationships were observed among patients with n0 disease.

These results indicate that p1 and p2 pleural involvement should be combined as a single category as VPI. A tumor of 3 cm or less with p1 involvement should, unlike the JLCS classification, be classified as T2. Although the UICC classifies a tumor of greater than 3 cm as T2 regardless of pleural involvement, our results suggest p1 or p2 tumors of greater than 3 cm should be upgraded to T3 status (Table 3).

In conclusion, this study indicates that VPI should be defined as tumor extension beyond the elastic layer of the visceral pleura, regardless of its exposure on the pleural surface. A tumor of 3 cm or less with VPI should remain a T2 tumor, as presently occurs in the UICC staging system (but upgraded in the JLCS staging system to match the UICC system), and tumors of greater than 3 cm with VPI should be upgraded to T3 status in both staging systems. This modification would make the non–small cell lung cancer TNM classification system simpler and cleaner.

We thank Professor J. Patrick Barron (International Medical Communication Center, Tokyo Medical University) for reviewing the English manuscript.

References

1. Brewer LA, Bai AF, Little JN, Pardo GR. Carcinoma of the lung: practical classification of early diagnosis and survival treatment. *JAMA.* 1958;166:1149-54.
2. Mountain CF. Revisions in the International System for Staging Lung Cancer. *Chest.* 1997;111:1710-7.
3. The Japan Lung Cancer Society. General rule for clinical and pathological record of lung cancer. [in Japanese]. 5th ed. Tokyo: Kanehara; 1999.
4. Naruke T, Suemasu K, Ishikawa S. Surgical treatment for lung cancer with metastasis to mediastinal lymph nodes. *J Thorac Cardiovasc Surg.* 1976;71:279-85.
5. World Health Organization. The World Health Organization histological typing of lung tumors. 3rd ed. Geneva: World Health Organization; 1999.
6. Kaplan EL, Meier P. Non parametric estimation from incomplete observations. *J Am Stat Assoc.* 1958;53:457-81.
7. Peto R, Peto J. Asymptomatically efficient rank invariant test procedures. *J R Stat Soc [A].* 1972;135:185-207.
8. Ichinose Y, Yano T, Asoh H, Yokoyama H, Yoshino I, Katsuda Y. Prognostic factors obtained by a pathologic examination in completely resected non small-cell lung cancer. An analysis in each pathologic stage. *J Thorac Cardiovasc Surg.* 1995;110:601-5.
9. Manac'h D, Riquet M, Medioni J, Le Pimpec-Barthes F, Dujon A, Danel C. Visceral pleura invasion by non-small cell lung cancer: an underrated bad prognostic factor. *Ann Thorac Surg.* 2001;71:1088-93.

Case Report

Late Pulmonary Metastasis of Renal Cell Carcinoma Resected 25 Years after Nephrectomy

Satoshi Shiono[1], Junji Yoshida[1], Mitsuyo Nishimura[1], Junichi Nitadori[1], Genichiro Ishii[2], Yutaka Nishiwaki[1] and Kanji Nagai[1]

[1]Department of Thoracic Oncology, National Cancer Center Hospital East and [2]Pathology Division, National Cancer Center Research Institute East, Kashiwa, Chiba, Japan

Received September 15, 2003; accepted December 6, 2003

A 50-year-old male underwent a left nephrectomy for clear cell type renal cell carcinoma (RCC) in February 1978. A right pulmonary metastasis was resected in February 1994. At that time, chest computed tomography revealed the presence of three small nodules in the left lung, but these were followed up as inflammatory lesions. In January 2002, a right pleural metastasis, which showed rapid growth, was detected and it was resected in June of the same year. A gradual growth was observed in the left lung nodules, and the patient underwent wedge resection of the left lung in March 2003, 25 years after nephrectomy. These nodules were diagnosed as metastatic RCC. Currently, the patient is doing well with no signs of recurrence, 8 months after the third metastasectomy.

Key words: renal cell carcinoma – late pulmonary metastasis – repeated metastasectomy – long disease-free interval

INTRODUCTION

Although pulmonary metastases of renal cell carcinoma (RCC) constitute the majority of cancer recurrences following nephrectomy, a disease-free interval of more than 20 years has rarely been reported. We previously reported an RCC patient with a metastatic pulmonary lesion resected 16 years after nephrectomy (1). During the postoperative follow-up, this patient underwent pleural metastasis extirpation in June 2002 and wedge resection of the left lung for pulmonary metastases in March 2003. To the best of our knowledge, the time interval between nephrectomy and metastasectomy is the longest ever reported in English literature from Japan. Therefore, this case is considered worthy of report.

CASE REPORT

A 50-year-old male underwent left nephrectomy for RCC at a university hospital on February 2, 1978. The disease was histopathologically diagnosed as RCC, clear cell type, grade 1, and stage I. In August 1989, an abnormal shadow was detected in the left lung, but it disappeared shortly. This shadow was diagnosed as pleuritis. In September 1993, an abnormal X-ray shadow was detected in an annual health check-up, and the patient was referred to our institution. Computed tomography (CT) revealed a small nodule in the right lung. Video-assisted thoracoscopic wedge resection of the right lung was performed in February 1994, 16 years after nephrectomy. Pathological examination revealed that the tumor was metastatic clear cell type RCC (1).

Chest CT performed before the resection also revealed the presence of small nodules in the left inferior lingular segment and posterior basal segment (Fig. 1a). These were diagnosed as inflammatory nodules following pleuritis, and we decided to use CT to follow them up. CT scans were performed annually, and a pleural tumor adjacent to the right superior and inferior segment was detected in January 2002 (Fig. 2a). Since this tumor showed rapid growth on CT in May 2002 (Fig. 2b), the patient underwent a video-assisted thoracoscopic extirpation of the parietal pleural tumor on June 18, 2002. Histopathological examination demonstrated an RCC metastasis.

CT performed in February 2003 revealed evident growth of the left lung nodules (Fig. 1b). No evidence of other recurrences was detected. On the basis of the diagnosis of RCC metastasized to the left lung, we planned a third resection.

The patient presented no symptoms at the time of the third admission in March 2003. Physical examination revealed surgical scars on the abdomen and right-sided chest wall.

For reprints and all correspondence: Junji Yoshida, Department of Thoracic Oncology, National Cancer Center Hospital East, 6-5-1, Kashiwanoha, Kashiwa, Chiba 277-8577, Japan. E-mail: jyoshida@east.ncc.go.jp

© 2004 Foundation for Promotion of Cancer Research

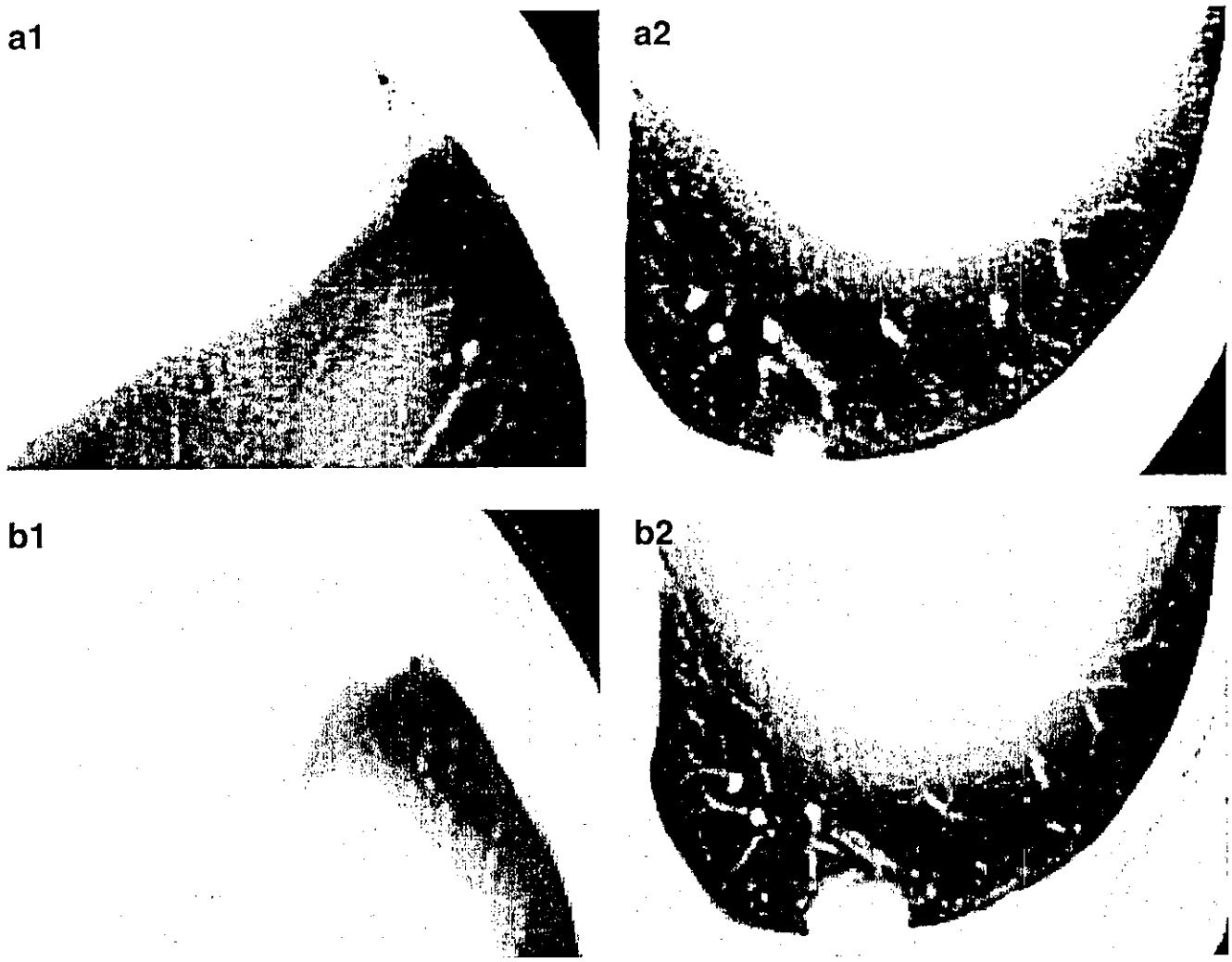

Figure 1. (a) Computed tomography, performed in November 1993, revealing small nodules in the left lung. (b) Computed tomography, performed in February 2003, revealing five nodules in the left lung. Evident growth was observed in the nodules.

Video-assisted thoracoscopic wedge resection of the left lung was performed on March 19, 2003, 25 years after nephrectomy. Three nodules were present in the left inferior lingular and posterior basal segment. These nodules were resected along with the surrounding normal pulmonary parenchyma using stapling devices. No other lesions were thoracoscopically evident.

In macroscopic findings, the resected lung specimen revealed yellowish protruding tumors, visible immediately beneath the pleural surface. Microscopically, the lesion consisted of tumor cells growing in an alveolar pattern, separated by stroma, characteristically endowed with prominent sinusoid-like vessels. The tumor cells had abundant clear cytoplasm and uniform small ovoid hyperchromatic nuclei (Fig. 3a). These histological features are similar to those of the previously resected metastatic lesions (Fig. 3b). The tumor was diagnosed to be compatible with metastatic clear cell type RCC.

The postoperative course was uneventful. The patient was discharged on the 7th postoperative day. Currently, the patient is doing well, with no signs of recurrence, 8 months after the third metastasectomy.

DISCUSSION

RCC frequently metastasizes to the lung. The prognosis of unresected metastatic RCC is poor. The 5-year survival rate of patients with metastatic RCC without surgical resection was only 9% (2). Chemotherapy, radiation therapy or immunotherapy has not proven effective for metastatic RCC. Surgical resection for pulmonary metastasis of RCC is a safe procedure (3–7). Complete surgical resection can result in long-term survival (5).

Piltz et al. (5) reported that the recurrence of resectable pulmonary metastases did not impair survival. This favors repeated resection. Pfannschmidt et al. (3) showed that the 5-year survival of patients undergoing repeated resection of pulmonary metastases did not differ from those with resection of a single metastatic lesion. Cerfolio et al. (4) stated that the 5-year survival rate of patients with repeated thoracotomy was similar